

Morphologies and Properties of Poly(phthalazinone ether sulfone ketone) Matrix Ultrafiltration Membranes with Entrapped TiO₂ Nanoparticles

Jin-Bo Li,^{1,2} Jie-Wu Zhu,¹ Mao-Sheng Zheng¹

¹School of Material Science and Technology, Xi'an Jiaotong University, Xi'an 710049, People's Republic of China

²Department of Science and Technology, Xi'an Shiyou University, Xi'an 710061, People's Republic of China

Received 23 February 2006; accepted 31 August 2006

DOI 10.1002/app.25428

Published online in Wiley InterScience (www.interscience.wiley.com).

ABSTRACT: Poly(phthalazine ether sulfone ketone) (PPESK) is a newly developed membrane material with superior thermal stability and comprehensive properties. Titanium dioxide (TiO₂)-entrapped PPESK ultrafiltration (UF) membranes were formed by dispersing uniformly nanosized TiO₂ particles in the casting solutions. Initially, the inorganic nanoparticles were organically modified with silane couple reagent to overcome the aggregation and to improve the dispersibility in organic solvent. The membranes were prepared through the traditional phase inversion method. The effects of inorganic TiO₂ nanoparticles on the membrane surface morphology and cross section structure were investigated using scanning electronic microscopy (SEM) and atomic force microscopy (AFM). Water contact angle (CA)

measurement was conducted to investigate the hydrophilicity and surface wettability of the membranes. The influence of TiO₂ on the permeability, antifouling, and tensile mechanical properties of the PPESK membranes were evaluated by UF experiments and tensile tests. The experimental results showed that the obtained TiO₂-entrapped PPESK UF membranes exhibit remarkable improvement in the antifouling and mechanical properties because of the introduction of TiO₂ nanoparticles. © 2006 Wiley Periodicals, Inc. *J Appl Polym Sci* 103: 3623–3629, 2007

Key words: poly(phthalazinone ether sulfone ketone); titanium dioxide; nanoparticles; ultrafiltration membrane; mechanical strength

INTRODUCTION

Membrane technology is receiving an increased attention in the fields of wastewater treatment, drinking water supply, protein separation, solute concentration, and so on. Synthetic polymers have widely been used as membrane materials since the first integrally asymmetric flat-sheet cellulose acetate membrane was developed by Loeb and Sourirajan.¹ For most synthetic membranes, membrane fouling during filtration is the major cause to result in a loss of membrane performances, especially permeation flux decline.² As a result of membrane fouling, the frequent cleaning or replacement of membrane modules leads to an increase of operation cost. Therefore, reducing or eliminating fouling has been a challenging problem in membrane application. Many efforts have been made to control membrane fouling, which generally was divided into three categories: the hydrophilic modification of membrane, pretreatment of

the feed solution, and optimization of membrane process.³ The blending hydrophilic additives with hydrophobic membrane materials is a convenient approach to improve the antifouling properties of a membrane. In recent years, inorganic nanometer particles has attracted great attention for the modification of separation membrane.^{4–6} Thereinto, nanosized titanium dioxide (TiO₂) is a prior candidate as additive for polymer membrane because of its high hydrophilicity, good chemical stability, innocuity, and ease of preparation.⁷

Poly(phthalazine ether sulfone ketone) (PPESK) is a novel amorphous copolymer whose chemical structure contains rigid phthalazine and aromatic rings, as shown in Figure 1. PPESK membrane behaves with high glass transition temperature (263–305°C), good chemical stability and solubility, also exhibits excellent comprehensive properties in gas separation, ultrafiltration (UF), and nanofiltration (NF).^{8–11} For example, several researchers reported a method of preparing PPESK composite NF membranes, and the obtained membranes were applied for separating dyes and salts from water at high operation temperature.^{12,13} Su et al. made use of chloromethylated PPESK to fabricate porous membrane through phase inversion method, and the membranes were quaternized in an aqueous solution of trimethylamine. The

Correspondence to: J.-B. Li (lijinbo6036@hotmail.com).

Contract grant sponsor: Tackling Key Problem of Shanxi Science and Technology Bureau; contract grant number: 2004K07-G12.

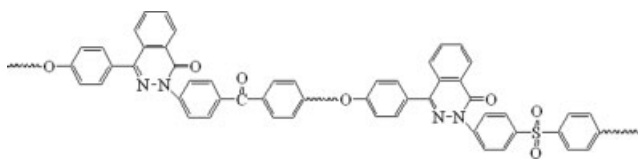


Figure 1 Chemical structure of poly(phthalazine ether sulfone ketone) (PPESK).

final membranes were used for the separation of dye and divalent salt from aqueous solutions.¹⁴ Wu et al. produced a composite membrane by interfacial polymerization of *m*-phenylene diamine and trimesoyl chloride on PPESK UF membrane for wastewater treatments.¹⁵ Despite its advantages as a membrane material, the hydrophobic character of PPESK is disadvantageous for the filtration of aqueous solution. The adsorption of protein and natural organic matter can lead to serious membrane fouling, thus a decline of permeation flux. So, it is significant to improve the hydrophilicity and antifouling properties of PPESK UF membrane.

Nano-TiO₂ has attracted much interest in the modification of porous membrane. Luo et al. performed the hydrophilic modification of polyethersulfone (PES) UF membrane through a self-assembly of TiO₂ nanoparticles on the membrane surfaces, and the resultant membranes exhibit good separation properties.¹⁶ Bae et al. prepared a variety of modified poly(vinylidene fluoride) (PVDF), polysulfone (PSf), and polyacrylonitrile (PAN) UF membranes by TiO₂ deposited or entrapped on these membranes, and it was found that membrane fouling was mitigated when the modified membranes were applied for activated sludge filtration in membrane bioreactors.¹⁷ After an organic surface modification, TiO₂ has good compatibility with some polar organic solvents such as *N,N'*-dimethylacetamide (DMAc), *N*-methyl-2-pyrrolidinone (NMP). So nanosized TiO₂ can homogeneously disperse in PPESK casting solution without aggregation.¹⁸ The objective of this work is to prepare a novel UF membrane by uniformly dispersing nano-TiO₂ particles in PPESK polymer matrix. The effects of the addition of TiO₂ on the membrane morphologies and properties were investigated by SEM, AFM analysis, UF experiments, contact angle measurements, tensile tests, and so on.

EXPERIMENTAL

Materials and reagents

PPESK (S : K = 1 : 1, $[\eta] = 0.65$ dL/g) as membrane material was provided by Dalian New Polymer (People's Republic of China). Nanosized TiO₂ particles (rutile type, average particle size of 30 nm) and silane couple reagent (KH550) were kindly

obtained from Hangzhou Dayang Nanotechnology (People's Republic of China). *N*-methyl-2-pyrrolidone (NMP), as solvent, is commercially analytical grade. Poly(vinyl pyrrolidone) (PVP, K30, Sinapharm Group) was used as additive. Bovine serum albumin (BSA, MW 67,000), chicken egg albumin (CEA, MW 45,000), and lysozyme (MW 14,400) were supplied by Bio Life Science and Technology (Shanghai, People's Republic of China). All other chemicals used in the experiments were commercially analytical grade.

Membrane preparation

A surface modification of nano-TiO₂ powders was conducted to improve the compatibility and dispersion in organic solvent following a reported procedure.¹⁹ A certain amount of silane couple reagent (KH550) was added into a suspension of TiO₂ (50 g/L, pH = 4.0). The mass ratio of KH550/TiO₂ in the mixture was about 1 : 50. After 6 h of vigorous stirring at 80°C, the mixture was centrifuged and fully washed with ethanol. The final product was isolated and dried for use.

TiO₂-entrapped PPESK UF membranes were prepared using phase inversion method. Casting dopes was prepared by adding the modified nano-TiO₂ particles to a solution with 15 wt % of PPESK and 4 wt % of PVP. The amount of TiO₂ varied as 0, 1, 2, and 3 wt % by weight of the solution, and these samples were labeled as PPESK-0, PPESK-1, PPESK-2, and PPESK-3, respectively. The dopes were vigorously stirred and ultrasonic vibrated to obtain uniform and homogeneous casting suspensions. After filtered and vacuum degassed, an appropriate amount of the suspension was cast on a glass plate at ambient atmosphere. After exposed in air for 30 s, the glass plate was immersed into an ethanol/water (30/70 v/v) bath. After complete coagulation and washing, the membranes were used for characterization.

Membrane characterization

A field emitting scanning electron microscopy (SEM; SIRION-100, FEI, Netherlands) and an atomic force microscopy (AFM; SPA 400, Seiko instrumental, Japan) were used to examine the surface morphologies and cross section structures of the membranes. For SEM examination, each cross section was prepared by fracturing the membrane in liquid nitrogen to avoid destroying membrane structure. All samples were sputtered with metallic gold before being placed into the sample room of SEM. AFM images were acquired in the tapping mode with silicone tip cantilevers having a force constant of 20 mN/cm.

To evaluate the hydrophilicity and surface wettability of the membrane, water drop (volume = 1.0 μ L) permeation process on the porous membrane surface

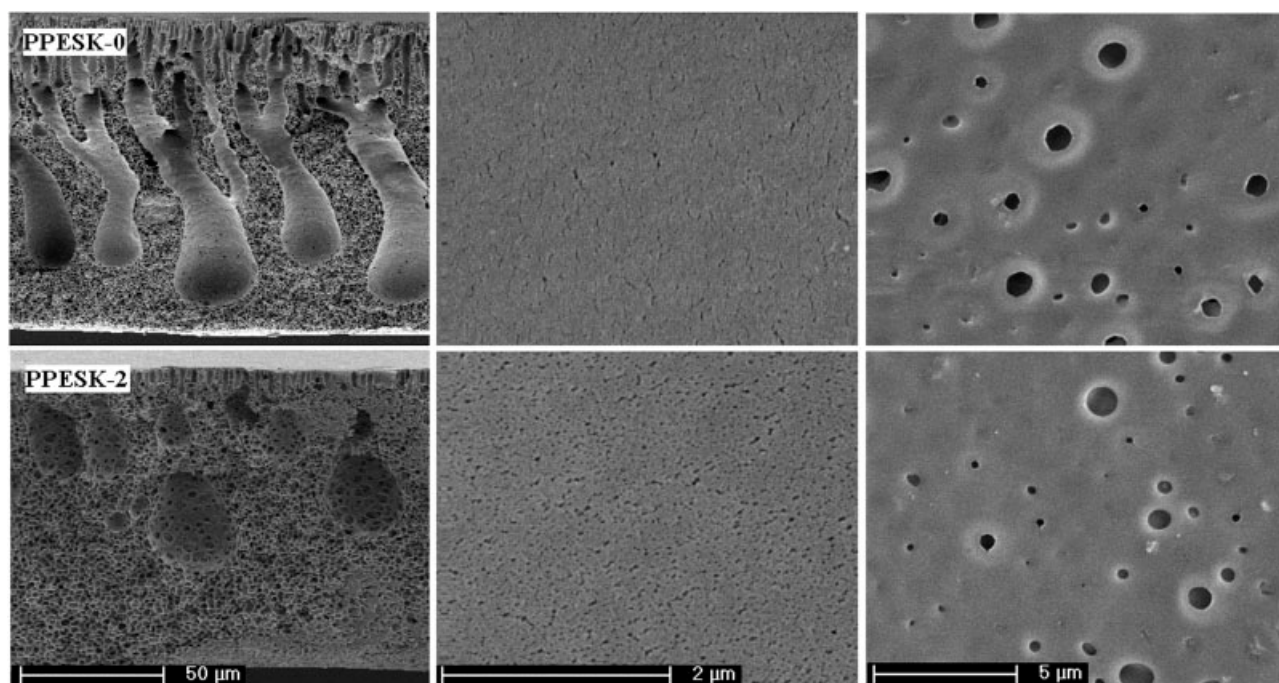


Figure 2 SEM images of the cross section, the top surface and the bottom surface of the membranes PPESK-0 and PPESK-2.

was analyzed with an OCA20 contact angle system (Dataphysics Instruments GmbH, Germany). It was performed on the top and the bottom surface for each membrane, respectively. The ambient conditions were 25°C and 60% relative humidity.

Pure water permeation flux and solute rejection were measured following a usual procedure. The wet membranes were compacted for 30 min at 0.15 MPa. Pure water flux was measured at 0.1 MPa after the flux reached steady state. The flux, J_{w0} , was calculated following the equation: $J_{w0} = V/(A \times t)$, where V is the total filtrate volume within the operation time t and A is the membrane area. Three protein aqueous solutions of BSA, CEA, and lysozyme with the concentration of 500 ppm were used for solute rejection measurements. The measurements were performed at room temperature and 0.1 MPa. The rejection, R , was expressed as: $R = (1 - C_p/C_f) \times 100\%$, where C_p and C_f are the solute concentration in the filtrate and feed, separately. Protein concentration in the feed and filtrate were measured with a spectrophotometer (Shimadzu, UV-1601, Japan).

The dynamic antifouling properties of the membranes were evaluated by the protein filtration experiments.²⁰ The tests were performed in a dead ended ultrafiltration cup fed with 1 g/L of BSA solution at 0.1 MPa. After 90 min of filtration, the permeate flux was recorded and labeled as J_p . Then the membrane was rinsed with deionized water for 10 min and the pure water flux was measured again (J_{w1}). At last, the membrane was washed with 0.05%

NaOCl solution for 10 min and the pure water flux was reevaluated (J_{w2}).

Tensile mechanical properties of the PPESK membranes were determined with an electronic tensile test machine (shimadzu, AG-1, Japan) at a crosshead speed of 2 mm/min.

RESULTS AND DISCUSSION

Morphologies and structures of membranes

The effects of nano-TiO₂ addition on the membrane surface morphologies and cross section structures were analyzed by SEM and AFM. Figure 2 shows the SEM images of the cross section, the top surface, and the bottom surface of the membranes PPESK-0 and PPESK-2, respectively. The cross section of both membranes displays a typical asymmetric morphology with macrovoids linked by sponge-like skin layers. With the introduction of TiO₂ into the casting dopes, the number of macrovoids of the membrane decreases, while the thickness of the skin layer increases. And, the length of finger-like pores in the sublayer becomes shorter. Comparison to the unmodified membranes, the top surface of the modified membranes shows a more porous skin layer structure due to TiO₂ addition. No apparent difference was founded at the bottom surfaces. As nano-TiO₂ particles has a large specific area and high surface energy, the addition of TiO₂ leads to a remarkable increase in the viscosity of casting dopes. Conse-

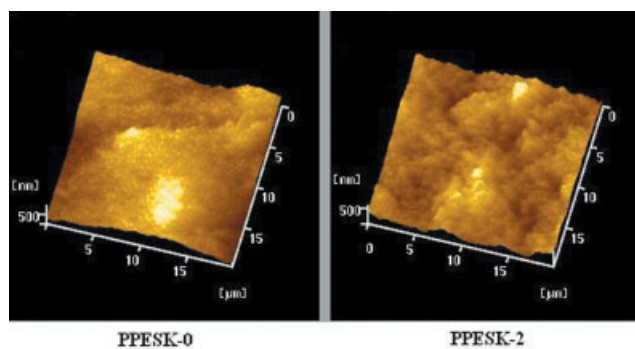


Figure 3 AFM 3-dimensional pictures of the top surface of the membranes. [Color figure can be viewed in the online issue, which is available at www.interscience.wiley.com.]

quently, the exchange rate of solvent–nonsolvent slows down and a delayed de-mixing might occur. The formation and growth of macrovoids in the membranes are suppressed.⁷ No TiO₂ agglomerate was observed in the micrographs of the surfaces and cross section of PPEsk-2. This indicates that the aggregate phenomenon of TiO₂ nanoparticles is effectively eliminated by the surface modification with KH550. TiO₂ were uniformly embedded inside the membranes.

The three-dimensional AFM images of the top surface of the membranes PPEsk-0 and PPEsk-2 are presented in Figure 3. The number of nodular aggregates of TiO₂-entrapped membranes is obviously bigger than that of the unmodified membranes. The roughness of the membranes notably increases with the TiO₂ concentration. In the range of scan area $20 \times 20 \mu\text{m}^2$, the root mean square (RMS) roughness of PPEsk-2 and PPEsk-0 are 165.8 and 91.3 nm, respectively. Mean pore size of the membrane surface was calculated by visual inspection of line profiles of different pores from various AFM images of different areas of the same membrane as described by Singh et al.²¹ The calculating values of mean pore size for PPEsk-2 and PPEsk-0 are 45.4 ± 1.52 nm and 27.9 ± 1.26 nm, respectively. It indicates that the introduction of TiO₂ contributes the membranes with a more porous skin layer. This result is in agreement with the observation of SEM.

Hydrophilicity and surface wettability

Contact angle measurements have been commonly used to characterize the polarity or surface energy of polymers. Such measurements are difficult to interpret for porous membrane due to capillary forces within pores, contraction in the dried state, heterogeneity, roughness, and restructuring of the surface. However, the relative hydrophilicity of membrane surface can be obtained by water contact angle measurement.²² For hydrophilic porous membrane, static

contact angle measurement was difficult to perform as the water drop disappeared into the membrane very soon. So a series of images of the water drop on the membranes were acquired in the movie mode and the curves of CA as a function of the drop age were plotted to compare the unmodified and modified membranes' hydrophilicity.^{23,24}

Figure 4 shows the curves of contact angle as a function of water drop age for the top surface of unmodified and TiO₂-entrapped PPEsk membranes. A remarkable difference was observed in the water contact angle of the membranes with different TiO₂ content. Generally, the higher amount of the added TiO₂ in the membranes, the lower is the contact angle. This result indicates that the addition of TiO₂ contributes the membrane with better surface wettability. For all membranes, the contact angle has an apparent declining trend with the drop age. The contact angle on the unmodified membrane attenuates very slowly, while that on the modified membranes, it changes more rapidly. And, the attenuation speed of contact angle increases with the TiO₂ concentration in the membranes. This phenomenon shows the hydrophilicity of the pores inside the membrane, is also improved by TiO₂ addition.

The changes of water contact angle with drop age on both surfaces of the membranes PPEsk-0 and PPEsk-2 were presented in Figure 5. For both the modified and unmodified membranes, contact angle on the top surface was lower than that on the bottom surface. At the drop age of 120 s, the contact angle on the top surface of PPEsk-0 was 81.0°, while that of PPEsk-2 was 15.6°, a decrease of 65.4°. But on the bottom surface, the contact angle difference at the drop age of 120 s between PPEsk-0 and PPEsk-2 was about 43.2°. It is showed that the wettability of the top surface was improved more drastically

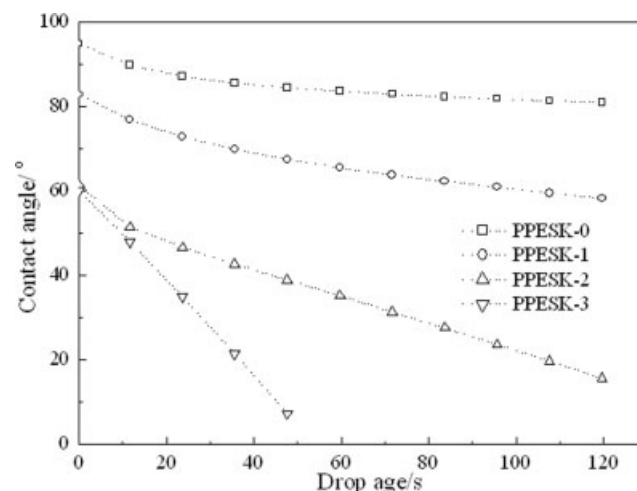


Figure 4 Changes of water contact angle with drop age on the top surface of the membranes.

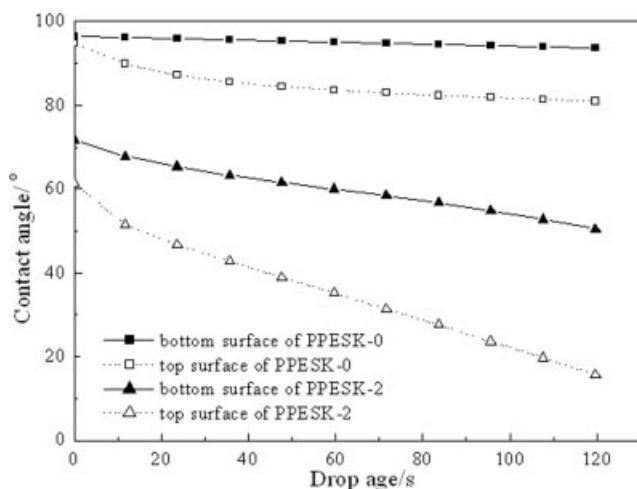


Figure 5 Changes of water contact angle with drop age on both surfaces of the membranes PPESK-0 and PPESK-2.

than that of the bottom surface. This phenomenon might be attributed to the accumulation of hydrophilic TiO_2 nanoparticles on the top surface during the phase inversion of membrane formation. Because of high surface energy and large specific surface area, TiO_2 preferentially segregates to the interface between the membrane and water.²⁵

Permeability and solute rejection

It is well known that the hydrophilicity of membrane can affect the permeation properties. To investigate the effect of TiO_2 addition on the permeability and separation performances of the PPESK membranes, pure water flux and solute rejection were measured under a transmembrane pressure of 0.1 MPa. As presented in Figure 6, the increase of TiO_2 concentration in the <2 wt % range results in an increase of pure water flux. Nevertheless, when the concentration is up to 3 wt %, the flux exhibits a declining trend. The enhancement of membrane permeability at a lower amount of TiO_2 is mainly owed to the improvement of membrane hydrophilicity and the change of membrane structures. The addition of TiO_2 nanoparticles brings a more porous membrane surface and skin layer, reducing the resistance of water permeation through the membranes. Meanwhile, the better hydrophilicity can attract water molecules into the membrane and decrease the interface tension of membrane-water, consequently endow the membrane with a bigger flux. When TiO_2 concentration was more than 3 wt %, the flux of the membranes was not improved. The contribution of hydrophilicity to the flux is weakened because of the aggregation phenomenon of a higher amount of nanoparticle, while the membrane morphology with a thicker skin layer and a compact sponge-like sublayer has a negative

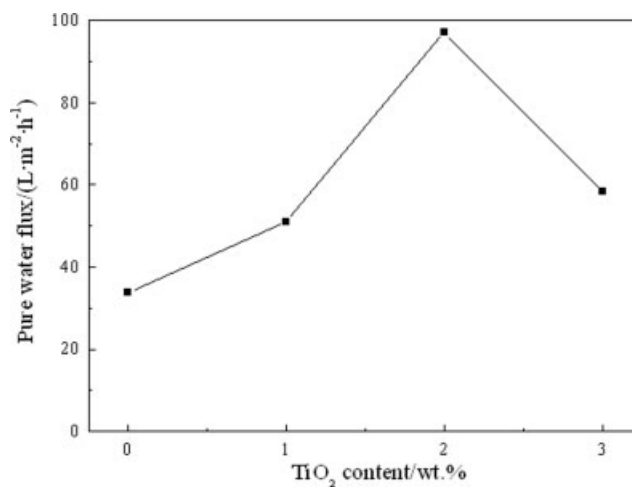


Figure 6 Pure water fluxes as a function of TiO_2 content in the PPESK membranes.

influence on the flux.⁷ So the amount of TiO_2 in the casting dopes should be properly controlled lower than 3 wt %.

Figure 7 presents the rejections of the membranes with different TiO_2 concentration against BSA, CEA, and lysozyme, respectively. For different membranes, the rejection against BSA is ~96% and has only a little difference among each other. The rejection against CEA and lysozyme of the membranes with 1 and 2 wt % TiO_2 has an increase than that of the unmodified membrane. The membrane structure with a thick skin layer is the main cause to the increase of solute rejection. However, the solute rejection for the membrane with TiO_2 concentration of 3 wt % shows a lower degree when compared with the membrane with 2 wt % TiO_2 . This might be attributed to the formation of large pores or flaws in the membrane caused by the nanoparticle aggregate

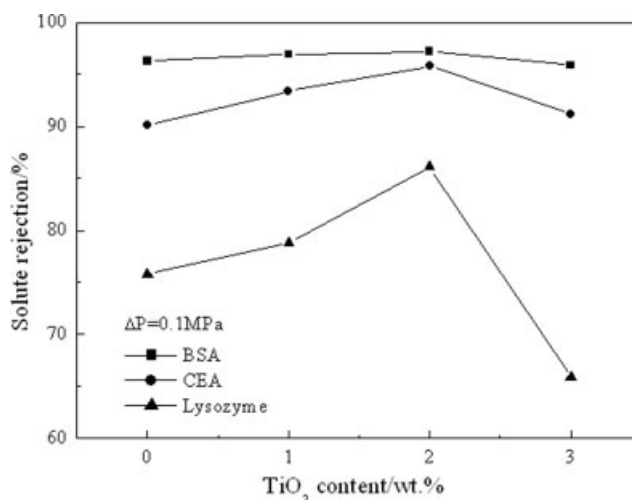


Figure 7 Solute rejections of the PPESK membranes with different TiO_2 content.

TABLE I
Protein Filtration Fluxes of the Membranes

Membrane	J_{w0} (L/m ² h)	J_p (L/m ² h)	J_{w1} (L/m ² h)	J_{w2} (L/m ² h)
PPESK-0	41.9	12.5	21.9	28.1
PPESK-1	50.4	16.7	29.3	36.9
PPESK-2	73.5	28.1	46.7	56.3
PPESK-3	54.2	25.9	38.1	46.2

J_{w0} , the initial pure water flux; J_p , BSA solution flux after 90 min of protein filtration; J_{w1} , pure water flux after water washing; and J_{w2} , pure water flux after chemical washing.

phenomenon because of the addition of excessive TiO₂.

Evaluation of antifouling properties

Membrane fouling is a major obstacle for a pressure-driven membrane used in industrial separating process. For efficient use in various applications, membrane fouling should be reduced as much as possible. The UF experiments using 1 g/L of BSA solution were performed to investigate the antifouling properties of the TiO₂-entrapped PPESK membranes. The values of flux in the protein solution filtration are listed in Table I. From the initial pure water flux, J_{w0} , and the protein solution flux, J_p , the degree of membrane fouling can be characterized by the relative flux reduction: $1 - J_p/J_{w0}$. The flux recovery ratios after water washing and chemical washing are defined as J_{w1}/J_{w0} and J_{w2}/J_{w0} , respectively.²⁶ The obtained results are presented in Figure 8. The value of $1 - J_p/J_{w0}$ decreased with the increase of the added TiO₂ amount, while that of J_{w1}/J_{w0} and J_{w2}/J_{w0} exhibited an increasing trend. The relative flux reduction ($1 - J_p/J_{w0}$) of the PPESK-3 membrane

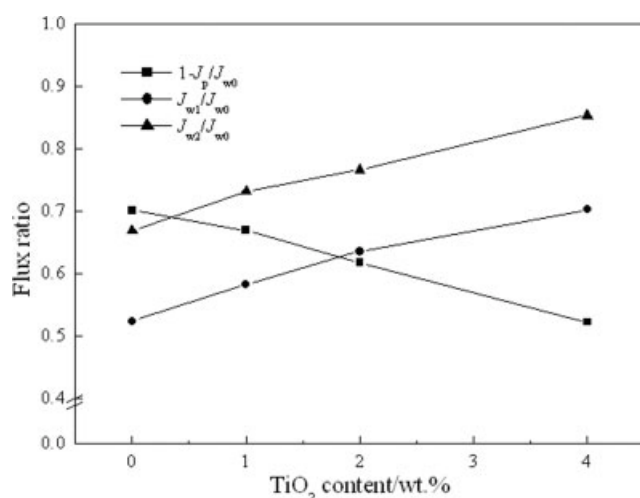


Figure 8 Effects of TiO₂ addition on the antifouling properties of the PPESK membranes.

is 25.5% lower than that of the unmodified membrane. It is showed that the PPESK membranes with entrapped TiO₂ are less susceptible to fouling than the neat membrane. Similarly, the values of flux recovery ratios, J_{w1}/J_{w0} and J_{w2}/J_{w0} , increased from 0.52 to 0.70 and 0.67 to 0.85, respectively, exhibiting the same change trend as membrane hydrophilicity. The results suggest that the protein fouling in the modified membranes was reversible and easily eliminated by water washing and chemical washing. It is concluded that the antifouling properties of the PPESK membranes were improved by TiO₂ addition.

Tensile mechanical properties

Tensile mechanical strength is an important parameter for membrane application. The typical curves of tensile strength tests for the membranes are shown in Figure 9, and the corresponding results are listed in Table II. Both maximum stress and break stress was remarkably elevated with an increase of TiO₂ content. The maximum stress increased from 3.98 MPa of the PPESK-0 membrane to 8.62 MPa of the PPESK-3 membrane, an increase of 117%. Similarly, the break stress increased from 3.98 to 7.01 MPa. These data shows that adding appropriate amount of nanometer-TiO₂ into the casting solution greatly enhanced the tensile strength of the PPESK membranes. The maximum strain and break strain firstly increased with the addition of inorganic nano-sized particles and presented a peak value at TiO₂ content of 1 wt %, then declining when more nanoparticles was added. It indicates that the membrane is more brittle and has less toughness due to the addition of rigid inorganic particles.

It is thought that the interaction of amorphous PPESK chains was significantly enhanced by the

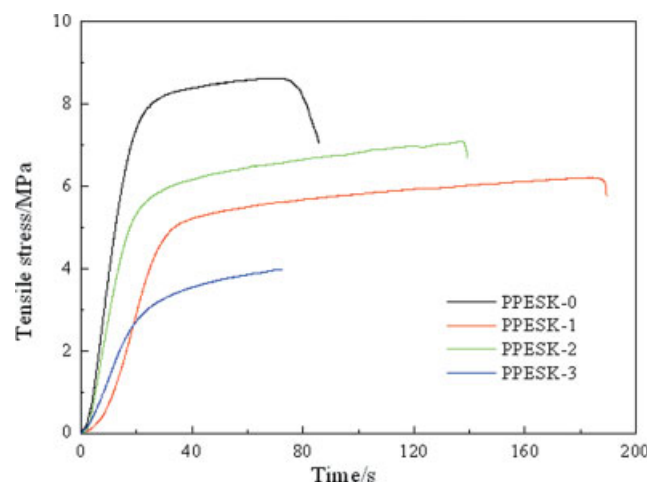


Figure 9 Curves of tensile strength tests of the membranes. [Color figure can be viewed in the online issue, which is available at www.interscience.wiley.com.]

TABLE II
Tensile Mechanical Properties of the Membranes

Membrane	Max stress (MPa)	Break stress (MPa)	Max strain (%)	Break strain (%)
PPESK-0	3.98	3.98	11.98	11.98
PPESK-1	6.23	5.75	30.60	31.62
PPESK-2	7.13	6.58	23.15	22.96
PPESK-3	8.62	7.01	11.54	16.27

inorganic nano-sized TiO₂ particles having a large specific surface area. At the same time, there exists a strong interaction between the inorganic particles and polymer matrix.⁷ Furthermore, the membrane structure holds a thicker skin layer and more sponge-like pores after TiO₂ being added into the casting dopes. All these factors contribute the membrane with higher mechanical strength.

CONCLUSIONS

In the present study, PPESK ultrafiltration membrane was modified by uniformly dispersing inorganic TiO₂ nanoparticles in the PPESK casting solution. The membranes were fabricated by the traditional phase inversion technique. The membrane morphologies and structure analysis using SEM and AFM indicates that the addition of TiO₂ contributes the membranes with a thicker and more porous skin layer. The membrane hydrophilicity and surface wettability was enhanced due to the introduction of hydrophilic TiO₂ particles. Permeability and rejection experiments showed that the pure water flux and solute rejection of the membranes were remarkably elevated when less amount of TiO₂ was added. Protein filtration experiments showed that the improved hydrophilicity contributed the membranes with better dynamic antifouling properties. Significantly, the tensile mechanical strength of membrane is also enhanced by TiO₂ addition.

References

- Loeb, S.; Sourirajan, S. *Adv Chem Ser* 1963, 38, 117.
- Taniguchi, M.; Belfort, G. *J Membr Sci* 2004, 231, 147.
- Sheikholeslami, R. *Desalination* 1999, 123, 45.
- Kwak, S. Y.; Kim, S. H.; Kim, S. S. *Environ Sci Technol* 2001, 35, 2388.
- Kim, S. H.; Kwak, S. Y.; Sohn, B. H.; Park, T. H. *J Membr Sci* 2003, 211, 157.
- Lu, Y.; Yu, S. L.; Chai, B. X. *Polymer* 2005, 46, 7701.
- Yang, Y.; Wang, P.; Zheng, Q. Z. *J Polym Sci Part B: Polym Phys* 2006, 44, 879.
- Jian, X. G.; Dai, Y.; Li, Z.; Xu, R. X. *J Appl Polym Sci* 1999, 71, 2385.
- Jian, X. G.; Dai, Y.; He, G. H.; Chen, G. H. *J Membr Sci* 1999, 161, 185.
- Qin, P. Y.; Chen, C. X.; Han, B. B.; Takuji, S.; Li, J. D.; Sun, B. H. *J Membr Sci* 2006, 268, 181.
- Wei, J.; Jian, X. G.; Wu, C. R.; Zhang, S. H.; Yan, C. *J Membr Sci* 2005, 256, 116.
- Dai, Y.; Jian, X. G.; Liu, X. M.; Guiver, M. D. *J Appl Polym Sci* 2001, 79, 1685.
- Zhang, S. H.; Jian, X. G.; Dai, Y. *J Membr Sci* 2005, 246, 121.
- Su, Y.; Jian, X. G.; Zhang, S. H.; Wang, G. Q. *J Membr Sci* 2004, 241, 225.
- Wu, C. R.; Zhang, S. H.; Yang, D. L.; Wei, J.; Yan, C.; Jian, X. G. *J Membr Sci* 2006, 279, 238.
- Luo, M.-L.; Zhao, J.-Q.; Tang, W.; Pu, C.-S. *Appl Surf Sci* 2005, 249, 76.
- Bae, T.-H.; Tak, T.-M. *J Membr Sci* 2005, 249, 1.
- Zhang, Z. H.; Shen, Z.; Shao, C. S. *China Surf Detergent Cosmet* 1997, 5, 13.
- Yao, C.; Ding, Y. H.; Lin, X. P.; Yang, X. J.; Lu, L. D.; Wang, X. *Chin J Inorg Chem* 2005, 21, 638.
- Pieracci, J.; Wood, D. W.; Crivello, J. V.; Belfort, G. *Chem Mater* 2000, 12, 2123.
- Singh, S.; Khulbe, K. C.; Matsuura, T.; Ramamurthi, P. *J Membr Sci* 1998, 142, 111.
- Shim, J. K.; Na, H. S.; Lee, Y. M.; Huh, H.; Nho, Y. C. *J Membr Sci* 2001, 190, 215.
- Steen, M. L.; Jordan, A. C.; Fisher, E. R. *J Membr Sci* 2002, 204, 341.
- Wavhal, D. S.; Fisher, E. R. *J Membr Sci* 2002, 209, 255.
- Ishihara, K.; Fukumoto, K.; Iwasaki, Y.; Nakabayashi, N. *Biomaterials* 1999, 20, 1545.
- Wavhal, D. S.; Fisher, E. R. *Langmuir* 2003, 19, 79.